Atmos. Chem. Phys. Discuss., 10, 8515–8551, 2010
www.atmos-chem-phys-discuss.net/10/8515/2010/

Atmospheric Chemistry and Physics Discussions

This discussion paper is/has been under review for the journal Atmospheric Chemistry and Physics (ACP). Please refer to the corresponding final paper in ACP if available.

GOMOS ozone profile validation using ground-based and balloon sonde measurements

J. A. E. van Gijsel[1], D. P. J. Swart[1], J.-L. Baray[2], H. Bencherif[2], H. Claude[3], T. Fehr[4], S. Godin-Beekmann[5], G. H. Hansen[6], P. Keckhut[7], T. Leblanc[8], I. S. McDermid[8], Y. J. Meijer[4], H. Nakane[9], E. J. Quel[10], K. Stebel[6], W. Steinbrecht[3], K. B. Strawbridge[11], B. I. Tatarov[12], and E. A. Wolfram[10]

[1]National institute for public health and the environment (RIVM), Centre for enviromental monitoring, Bilthoven, The Netherlands
[2]University of La Réunion, Saint Denis, France
[3]German weather service (DWD), Hohenpeissenberg, Germany
[4]European space agency (ESA-ESRIN), Frascati, Italy
[5]CNRS/UPMC/UVSQ, Paris, France
[6]Norwegian air research institute (NILU), Tromsø, Norway
[7]Laboratoire atmosphères, milieux, observations spatiales (LATMOS), Verrières-le-Buisson, France
[8]Jet Propulsion Laboratory, California Institute of Technology, Table Mountain Facility, Wrightwood, USA

[9]National institute for environmental studies, Asian environment research group, Tsukuba, Japan
[10]Laser and applications research centre (CEILAP), CITEFA-CONICET, Villa Martelli, Argentina
[11]Science and technology branch, Environment Canada, Centre for atmospheric research experiments, Egbert, Canada
[12]National Institute for Environmental Studies, Atmospheric remote sensing section, Tsukuba, Japan

Received: 31 January 2010 – Accepted: 21 March 2010 – Published: 1 April 2010

Correspondence to: J. A. E. van Gijsel (anne.van.gijsel@rivm.nl)

Published by Copernicus Publications on behalf of the European Geosciences Union.

Abstract

The validation of ozone profiles retrieved by satellite instruments through comparison with data from ground-based instruments is important to monitor the evolution of the satellite instrument, to assist algorithm development and to allow multi-mission trend analyses.

In this study we compare ozone profiles derived from GOMOS night-time observations with measurements from lidar, microwave radiometer and balloon sonde. Collocated pairs are analysed for dependence on several geophysical and instrument observational parameters. Validation results are presented for the operational ESA level 2 data (GOMOS version 5.00) obtained during nearly seven years of observations and a comparison for a smaller dataset from the previous processor (version 4.02) is also included.

The profiles obtained from dark limb measurements when the provided processing flag is properly considered match the ground-based measurements within ±2% over the altitude range 20 to 40 km. Outside this range, the pairs start to deviate more and there is a latitudinal dependence: in the polar region (higher amount of straylight contamination), differences are start to occur lower in the mesosphere than in the tropics, whereas for the lower part of the stratosphere the opposite happens: the profiles in the tropics reach less far down as the signal reduces faster because of the higher altitude at which the maximum ozone concentration is found compared to the mid and polar latitudes. Also the bias is shifting from mostly negative in the polar region to more positive in the tropics

Profiles measured under "twilight" conditions are often matching the ground-based measurements very well, but care has to be taken in all cases when dealing with "straylight" contaminated profiles.

For the selection criteria applied here (data within 800 km, 3 degrees in equivalent latitude, 20 h (5 h above 50 km) and a relative ozone error in the GOMOS data of 20% or less), no dependence was found on stellar magnitude, star temperature, nor the

ACPD

10, 8515–8551, 2010

azimuth angle of the line of sight. No evidence of a temporal trend was seen either in the bias or frequency of outliers, but a comparison applying less strict data selection criteria might show differently.

1 Introduction

1.1 Background

Ultraviolet light (UV) present in solar radiation can potentially threaten life on Earth as UV radiation can cause alterations in DNA (Luchnik, 1975). Ozone in the Earth's atmosphere absorbs 97 to 99% of the UV, significantly reducing the harmful effects. Most of these absorption reactions take place in the so-called ozone layer, which is located at altitudes between 15 and 35 km. A reduction of the ozone concentration and associated increase of the ultraviolet radiation is expected to result in a change of plant species composition and a possible reduction of agroecosystem production (Milchunas et al., 2004; Ballare et al., 1996; Koti et al., 2005). Another example from animal experiments suggests that through the increase of UVb radiation (between 280 and 315 nm), for each 1% loss of ozone the incidence of cataract would rise by 0.5% (van der Leun and de Gruijl, 1993) and from epidemiological data an increased incidence of non-melanoma skin cancer by 2% can be expected per percent ozone decrease (Urbach, 1997).

The catalytic destruction of ozone by chlorofluoromethanes was first described by Molina and Rowloand (1974). In order to protect Earth's life from the UV, the so-called the Montreal protocol was designed to protect the ozone layer from destruction by ozone depleting substances. Although production of these substances has been significantly reduced, due to their long life-time ozone destruction will still continue for several years, as can be seen from the appearance of the record-size ozone hole above Antarctica in 2006 (ESA, 2006).

ACPD
10, 8515–8551, 2010

The European Space Agency launched the ENVISAT satellite dedicated to environmental research in March 2002. ENVISAT carries three instruments dedicated to atmospheric studies: SCIAMACHY, MIPAS and GOMOS (see http://envisat.esa.int/instruments/). The main objective of the last instrument is to monitor ozone and its trends in the stratosphere. GOMOS stands for Global Ozone Monitoring by Occultation of Stars and as its name states, this instrument uses stellar occultation to retrieve information on ozone and other trace gases from spectra in the ultraviolet, visible and near-infrared wavelengths. GOMOS is self-calibrating and due to its star tracking capabilities it has a very accurate altitude determination.

Approval has recently been given for the continuation of the ENVISAT mission beyond 2010 (its originally planned end of mission year). The current end of the mission is expected no later than August 2014, but the exact date depends on the available amount of fuel (EO-PE – PLSO and MAO teams, 2007). In order for the mission to continue, some orbital changes will take place in October 2010. These changes will reduce the altitude of the platform and reduce the repeat cycle from 35 to 30 days, but no major problems are foreseen for GOMOS acquisitions. However, comparison with long-term validation records is required to monitor the effects of these changes as well as the platform/instrument's ageing and to assess improvements in the GOMOS processing algorithms. In this respect, validation activities are essential to guarantee the stability of the quality of GOMOS and other remote sensor products (Dupuy et al., 2009; Brinksma et al., 2006).

1.2 Previous validation activities

The quality assessment of ozone profiles retrieved from satellite data can be carried out in three different ways: (1) using model studies/climatology; (2) using already validated alternative satellite products or (3) using profiles collected with ground-based/airborne instruments.

Bertaux et al. (2004) compared GOMOS ozone profiles of 4 days in 2002 with the Fortuin-Kelder ozone climatology and found an excellent agreement. Found differences

ACPD
10, 8515–8551, 2010

were attributed to natural variation and the inclusion of day-time data in the climatology whereas only night-time GOMOS measurements were taken for the comparison. They also compared two GOMOS measurements at the same location, but from two consecutive orbits and using distinct stars. The observed internal consistency was again referred to as “excellent”.

Verronen et al. (2005) compared night-time GOMOS ozone profiles with MIPAS measurements for individual cases as well as profile means for a limited number of profiles (1 day in 2002 and 1 day in 2003). Although MIPAS uses a different measurement technique from GOMOS (MIPAS is a mid-infrared limb sounder), good agreement – within 10–15% – was found for the stratosphere and lower mesosphere. Nevertheless, MIPAS persistently gives a higher estimate in this altitude region. Note that also two processor versions for GOMOS had been used for the different days.

In Meijer et al. (2004), a comparison of approximately 2500 GOMOS version 4.02 ozone profiles using data from lidar, balloon sonde and microwave radiometer data was presented. The authors illustrated that the quality of the GOMOS profiles strongly depended on the limb illumination conditions. For dark limb measurements, the GOMOS profiles agree well (bias < 7.5%) with the collocated data over the altitude range 14 to 64 km. No dependence on star temperature and magnitude or latitude was found, although the observed bias between 35 and 45 km was somewhat larger in the Polar Regions.

The ozone profiles delivered by GOMOS were compared with balloon sonde measurements acquired in 2003 at two locations by Tamminen et al. (2006). Their results indicated that the overall agreement between collocated measurements was good and that small scale structures could be detected with GOMOS’ vertical resolution. Explanations for the differences between the two locations were sought in star brightness and strength of the polar vortex.

For the tropical zone, several ground-based and satellite measurements including GOMOS have been compared with data from a balloon-based sensor (SAOZ UV-Vis spectrometer using solar occultation) circling the globe in three missions (Borchi and

ACPD
10, 8515–8551, 2010

Pommereau, 2007). GOMOS prototype processor version 6.0b performed very well above 22 km (bias of 1–2.5%), but degraded strongly below this altitude. Even though the altitude registration of GOMOS was considered very precise, SAGE II and SAOZ were found to be more precise (in terms of ozone): ∼2% compared to ∼6% for GOMOS above 22 km. Note however that the latitudinal coverage was very limited as well as the number of data samples. Furthermore, it is suggested that remote sensing measurements have a systematic high bias in oceanic convective clouds areas.

1.3 Outline

This article can be seen as a continuation of the work presented in Meijer et al. (2004) as the available GOMOS dataset is extended to seven years and a new processor version is available. The following sections will describe the used input data, and the methodology. Section three will present the validation results with in 3.1 the comparison between the previous processor (version 4.02) and the current operational processor (version 5.00) for an overlapping dataset and in 3.2 the validation results of version 5.00 for the seven-year-spanning dataset. The conclusions can be found in Sect. 4.

2 Data and methodology

2.1 GOMOS ozone profiles

The GOMOS data used in this study include the operational level 2 data from version 5.00 spanning the period August 2002 to August 2009. We also obtained a dataset processed with the previous algorithm version 4.02 for comparison purposes. This second set contains data from the period June 2004 to January 2005 complemented with a few measurements in August 2005. Note that as the version 4.02 data do not cover the same time period as used in Meijer et al. (2004), the results presented here are not directly comparable. We do not intend to reproduce their results; we merely aim

ACPD
10, 8515–8551, 2010

to point out differences between version 4.02 and 5.00 relative to the ground-/balloon-based measurements. Section 2.1.1 describes the implemented changes from the old (4.02) to the current (5.00) processor. All data were restricted to an estimated error in the ozone concentration of 20% or less.

The Product Confidence Data (PCD) flags in the GOMOS products indicate the validity of the retrieval of the local density profiles. In addition, the GOMOS ozone profiles receive a quality flag based on the illumination conditions of the atmospheric limb. Five illumination conditions have been characterised:

- bright (solar zenith angle at the tangent point smaller than 97° at an altitude lower than 50 km)
- twilight (not bright, solar zenith angle at the tangent point smaller than 110° at an altitude lower than 100 km)
- straylight (not in bright limb and solar zenith angle at the position of ENVISAT smaller than 120° during at least one measurement)
- twilight + straylight (not in bright limb, but twilight and straylight conditions both fulfilled)
- full dark (not in bright limb, straylight and/or twilight not fulfilled)

Because of the orbit chosen for ENVISAT, no full-dark measurements can be taken over the Arctic region. Nevertheless, similar to Meijer et al. (2004), an alternative filtering using a solar zenith angle larger than 108° (astronomical twilight zenith angle) for the tangent points will be tested here as well in order to get a picture for this region.

2.1.1 Changes from version 4.02 to 5.00

In addition to various corrections applied to the level 1 product, several level 2 processor changes have been implemented in IPF 5.00.

ACPD
10, 8515–8551, 2010

The atmospheric density profile is no longer retrieved in version 5.00; instead a reference atmospheric density profile is derived from ECMWF data and integrated into the version 5.00 retrieval. This was implemented as in version 4.02 a strong deviation from ECMWF data below 25 km and above 40 km was observed. The retrievals should especially improve at low altitudes where ECMWF data are accurate.

Additional errors are reported for ozone, NO_3 and aerosols. A quadratic aerosol law ($\alpha\lambda^2+\beta\lambda+\gamma$, with λ as the wavelength and α, β and γ as constants) has been incorporated to describe the wavelength dependence of the aerosol extinction, whereas in version 4.02 an inverse wavelength dependence $\left(\frac{1}{\lambda}\right)$ was assumed. A number of different aerosol models has been studied where the quadratic model showed the best performance in comparison to other satellite and ground-based measurements (GOMOS quality working group meeting 15, 2007).

A different cross section was introduced for the retrieval of ozone in IPF 5.00. Liu et al. (2007) have shown from testing different ozone cross sections with GOME UV measurements that a difference of up to 100% may be found in the values of the retrieved ozone profiles. In a study performed for the European Space Agency, Orphal (2002) recommended the use of Bogumil et al. (2000) for the visible wavelengths and Bass-Paur (1985) after application of some corrections in the UV region. Nevertheless, Bogumil et al. (2000) is used for both the UV and the visible wavelengths.

In the current implementation, the processor uses a linear function to interpolate the experimental data to other temperatures. Note that Orphal (2003), who has evaluated the effects on the ozone cross-section by the variation with temperature and the dependence on spectral resolution and wavelength shifts through comparison of various laboratory studies, recommended the use of a quadratic polynomial for this interpolation.

Despite the inaccuracies possibly introduced by these choices, the implementation of this cross-section had shown to significantly improve results in a verification study before the full mission re-processing with version 5.00 (Guirlet, personal communication, 2008).

ACPD
10, 8515–8551, 2010

2.2 Ground-based measurements

The importance of ground-based measurements is slowly getting recognised by initiatives like GAW (Global Atmospheric Watch), Geomon (Global Earth Observation and Monitoring of the atmosphere) and GMES (Global Monitoring for Environment and Security). Despite the fact that this kind of measurements is essential for a global understanding of our climate, securing long-term funding to warrant its continuation is usually rather difficult (Nisbet, 2007). Although satellite observations can complete the picture through the spatial coverage of their measurements, we must ensure a careful validation of the derived information. It is important to realise that satellite-based instruments are complementary to the ground-based observations as for instance the temporal and vertical resolutions of the last category are often higher and the error of the products better characterised. Furthermore, the long-term background measurements by ground-based observations are required to overcome data gaps in between of satellite missions and to quantify the introduced differences between sequential satellite-based instruments (McDermid et al., 1990; Jégou et al., 2008; Clerbaux et al., 2008).

2.2.1 Stratospheric ozone lidar data

In this study we make use of ozone profiles derived from differentially absorbed lidar signals emitted and recorded by stratospheric ozone lidar systems. Two light pulses are simultaneously emitted at different wavelengths with different ozone absorption cross sections. The difference in the returned backscatter can be related directly to the ozone concentration, which is derived as a function of the altitude based on the elapsed time since the pulse emission. The lidars mostly operate under night-time and clear-sky conditions.

All of the eleven participating lidars are part of the Network for the Detection of Atmospheric Composition Change (NDACC). The lidar working group of NDACC has developed various protocols to ensure consistency between the different lidars and high data quality is established through intercomparison and validation exercises with

models and other instruments (McDermid et al., 1998; NDACC lidar working group, 2009).

The data used in this study were restricted to an uncertainty of 30% or less, and to the altitude range 18 to 45 km.

2.2.2 Balloon-borne ozone sonde data

Ozone sondes consist of an inert pump, an electrochemical cell facilitating a reaction between ozone and iodide, a detector for the small electric current generated by this reaction, and an interface to a radiosonde for the measurement of air temperature and pressure (Deshler et al., 2008). Data are provided as partial ozone pressure, which under the assumption of a hydrostatic equilibrium can be converted to number density using the ideal gas law and the air temperature and pressure that were measured simultaneously to ozone by the sonde.

In this study, balloon soundings has been used from the Ground-Based Measurement and Campaign Database (GBMCD) subgroup of the Atmospheric Chemistry and Validation Team (ACVT) with the addition of Southern Hemisphere Additional Ozonesondes (SHADOZ, see Thompson et al., 2003a, b, for a description of this initiative) to increase the coverage in the tropics.

Data from the SHADOZ sondes are re-binned to longer time intervals using a block average for a given time window size (e.g. 10 s). In order to deal with the non-linear behaviour of pressure with increasing altitude, the logarithm of the reported pressures was taken before averaging, followed by taking the inverse logarithm of this average to normalise.

All sonde data has been cut off at an altitude of 30 km and averaged over two kilometer (corresponding to the GOMOS resolution below 35 km) to avoid the introduction of local biases caused by the presence of small scale structures seen by the sonde which would mainly enlarge the standard deviation of the differences.

ACPD
10, 8515–8551, 2010

2.2.3 Microwave radiometer data

As a third validation instrument we have used data from microwave radiometers. These instruments are often operated continuously during both day and night time. Although they have a broad vertical resolution, the data are useful to study the stratosphere and especially the mesosphere where lidar data are no longer available. Data are restricted in this study to altitudes ranging between 30 and 70 km with the condition that the reported error cannot exceed 30%.

2.3 Potential vorticity data

Potential Vorticity (PV) data on the 475 K potential temperature field were obtained from the ECMWF interim re-analysis (ERA-interim) data archive. Since it has been noted that the position of the vortex boundary derived from potential vorticity data may differ from that seen in observations (Greenblatt et al., 2002; Müller and Günther, 2003), which has been attributed to the availability of input data for the calculation of PV, it was decided not to interpolate the PV spatially and temporally nor to derive the vortex position. Instead, equivalent latitudes were derived for all GOMOS 5.00 data as well as for the ground-based measurements and data were linked to the nearest grid cell (cell size of 1.5°) and closest time (PV data are computed for 8 h intervals). Subsequently, the relative equivalent latitude difference between the GOMOS and ground-based measurements was used to study the effect on the validation results.

2.4 Collocations and data treatment

Following Meijer et al. (2004), we have restricted all collocations to a maximum horizontal distance of 800 km and a maximum time difference of 20 h between measurements. For the full dataset comparison in Sect. 3.2, we also enforce a maximum difference in equivalent latitude of 3 degrees to avoid problems in the polar region related to observing different air masses. Above altitudes of 50 km, the maximum time difference is

ACPD
10, 8515–8551, 2010

set to 5 h and the daylight conditions have to be the same, as mesospheric ozone is subject to diurnal variation.

Both the validation and GOMOS datasets have been interpolated using a linear spline to a common (200 m) altitude grid. As described before, the sonde data are averaged to the GOMOS resolution. Differences in vertical resolution are not taken into account for the lidar and microwave radiometer data. For the lidar data the effect is considered relatively small given the similar resolution of GOMOS. If we are to apply the averaging kernels and consider the a-priori information from the microwave radiometer data, the GOMOS data will be degraded and no longer independent from the microwave radiometer data (Meijer et al., 2003). The effect of not taking this resolution difference into account should lead to an increased standard deviation of the differences between GOMOS and the microwave retrievals. Substantial differences would be expected at altitude regions where there are small scale features, which is less likely above 30 km. Moreover, if we assume that the microwave radiometer smoothing error is stochastic, the mean error introduced by the difference in resolution should become zero when the dataset gets sufficiently large.

A complete validation should also consider the provided estimates of error in the ozone retrievals. In this study we have only used the provided errors in the validation and GOMOS data in the data selection process as for GOMOS the estimated error is subject of discussion in the quality working group (e.g. the scintillation correction is still an issue; Sofieva et al., 2009) and errors in the validation data are often not reported (sonde) or non-homogeneous (e.g. different definitions used in the lidar community). As a consequence, a full study could be dedicated to the comparison of errors and their uncertainties. We believe that through the large numbers used in the analyses, these complications are dealt with in a different way as the error in the data should correspond to the spreading seen in a dataset for a large population.

ACPD
10, 8515–8551, 2010

3 Analysis of the validation results

3.1 Comparison between versions 4.02 and 5.00

Figure 1 shows the comparison between GOMOS versions 4.02 (top) and 5.00 (bottom) with the validation data (VALID). The left panels of both plots show the mean ozone profiles (thick lines) as a function of altitude together with the corresponding standard deviations (thin lines) for GOMOS (in red) and the validation data (in blue). The ozone data is shown on a log-scale from 50 km upward to enhance visibility. The middle plots show the difference between GOMOS and the validation, where the difference is calculated as: $\frac{\text{GOMOS}-\text{VALID}}{\text{VALID}} \times 100$. The green line shows the median difference, the thick black line corresponds to the mean difference, the thin black lines illustrate the mean ±1 standard deviation and the thin grey lines show the mean ±2 standard errors. The number of used collocated pairs for a given altitude is shown on the right side of the middle panel, whereas the total number of collocated pairs is shown at the bottom of the panel. The right panel shows the following quantiles of the differences (lines from left to right): 2.5%, 16%, 50% (median), 86% and 97.5%.

The differences between the two analyses in total pairs and the collocated pairs for some altitudes originate from the difference in assigned errors to the datasets. In general more data points in version 5.00 fulfil the criterion of a maximum error of 20%.

Few outstanding differences between the two versions can be observed in the median profiles. The small negative bias from 20 to 50 km has shifted positively. With both versions, the standard deviation increases substantially below 30 km due to the presence of some outlier profiles. A large part of the deviation between the mean and median differences between 24 and 30 km can be attributed to comparisons with Dumont d'Urville (66.7° S), Thule (76.5° N) and Legionowo (52.4° N) soundings. A closer investigation at the latter two sites pointed out that some of these observations include straylight contamination. At Dumont d'Urville however, the illumination condition is not the only factor involved, as fully dark observations still produce outlier ozone concentrations compared to the soundings. This can be attributed to the increasing spatial

variability in this area as time progresses, given the fact that the June and July comparisons show good results. As ozone depletion can start already in mid-winter at the latitude of Dumont d'Urville (Roscoe et al., 1997), differences with measurements at other latitudes are likely to be found, which is what we observe in this case – with the relatively large distance between the (fully dark) satellite and sonde measurements. In addition, small scale structures are difficult to follow the with GOMOS' resolution. As spring advances, so does the ozone hole formation whereas the illumination conditions for GOMOS observations get worse. As a result, most collocations are with lower latitude measurements, which have a very different ozone distribution in this period. One future solution would be to optimise the collocation criteria latitude and/or time of the year dependent.

Figure 1 (see the GOMOS standard deviation in left panel) also shows that a few additional outlier profiles are produced with version 5.00 around the ozone maximum. These can be filtered out by removing unrealistic profiles exceeding a concentration of 10^{13} molecules per cm^3.

Note that differences with the comparison carried out by Meijer et al. (2004) at the higher part of the profile (above 45 km where only microwave data are available for comparison) in version 4.02 are caused by a difference in the time span of the their and our datasets: the current analysis only covers data from 2004 and 2005, resulting in fewer collocations with microwave radiometers and at fewer sites (e.g. no data is available for Lauder and Mauna Loa). In fact, the majority of these collocations are found at Payerne (80 to 95% depending on the altitude), making the top of the plot a rather local instead of global picture.

Figure 2 shows the same picture as Fig. 1 but with the outlier profiles removed as described above. The median difference profiles are, as expected, virtually the same. The mean now follows the median from an altitude of about 20 to around 60 km. Outside this range we still detect outliers due to a low signal to noise ratio and increased scintillation (low altitudes), whereas we will investigate with the longer and larger v5.00 dataset if the observed behaviour at higher altitudes is also seen at other locations.

ACPD
10, 8515–8551, 2010

3.2 Validation of the GOMOS 5.00 ozone profiles

In this section we present the validation results for all seven years. Note that more collocations are found in early years where funding was available for additional validation measurements, and secondly, GOMOS had a larger spatial coverage in the beginning as it could use a larger azimuth range for the line of sight.

We have split the main dataset into various subsets to identify possible dependencies on observation characteristics. Table 1 gives an overview of the used ranges for these parameters and Fig. 3 shows the locations of the GOMOS data together with the validation sites.

3.2.1 Illumination condition

Figure 4 shows the quality of the observations as a function of the illumination condition. The bright limb cases are presented on the left panel, showing that the retrieval with the current processor is still insufficient for these cases. At high altitudes there is a large negative bias and below 35 km the profiles contain many extreme values.

Under twilight conditions (middle panel), the results look a lot better. Compared to the full-dark limb cases (right panel), there are more high outliers, but a substantial amount of data can be used.

3.2.2 Stellar properties

Observations of strong stars should result in profiles of higher quality as the signal is less noisy. Indeed the 16% and 84% quantiles (Fig. 5) show a narrower distribution over a large part of the altitude range. However, the 97.5% quantile shows the presence of some high-value outliers. The number of collocations with strong stars is low in comparison to the weak stars-cases, making the difference profiles more variable. At altitudes above 45 km, the majority of the collocations are in the Polar region (Ny Ålesund microwave radiometer), whereas for the weak star observations most of the

ACPD
10, 8515–8551, 2010

collocations are located in the mid-latitude region. This explains why the difference profiles for the top appear worse for the strong star cases – when we consider only the polar cases, there is almost no difference between the two star magnitude groups.

With respect to the temperature of the observed stars, fewer collocations with cold stars are available than with hot stars, especially in the mesosphere. No significant influence of the star's temperature on the results was found. However, if we increase the maximum permitted error for GOMOS to 100%, then we see an increase in the number of available profiles, but the higher half of the profile (roughly above 40 km) shows a strongly increased variability and the median differences enhance with respect to the cases shown in Fig. 6 (e.g. at 55 km, the data has a negative bias of 50% and at 70 km the bias equals about 30% – not shown). Note that the mentioned data are not flagged invalid.

3.2.3 Line of sight azimuth angle

Figure 7 shows the influence of the Line Of Sight (LOS) azimuth angle during the time of observation. Most observations are found to be in slant viewing and quite a few (given the smaller azimuth range) are in the back LOS. The median difference profiles are very similar, but fewer outliers are observed in the back LOS configuration. Contrarily to Meijer et al. (2004), an increased standard deviation is not (any longer) seen for the side LOS data.

GOMOS is currently (January 2010) operating in the range 10° to 40°, which corresponds fully to the slant LOS. The past ranges are listed in the GOMOS monthly status reports, see http://earth.esa.int/pcs/envisat/gomos/reports/monthly.

3.2.4 Geographical area

For the analysis shown in Fig. 8 the dataset has been split into three geographical regions. Most collocations are found in the mid-latitude region (right panel), where the majority of the validation stations is located. In the polar region (left panel) there are

also many collocations: even though there are fewer stations, there are many GOMOS overpasses given the orbit of ENVISAT. This leads to various GOMOS measurements collocating with a single ground-based measurement. The collocating microwave data are from two stations: Ny Ålesund (largest contribution) and Kiruna (7 to 9 profiles above 55 km). The GOMOS profiles increasingly start to overestimate the ozone concentration above 50 km, which is likely an effect of the increasing straylight contamination. Perhaps the processor that is under development in the GOMOS bright limb project will improve the ozone retrieval as it does not depend on the weak star signals. In comparison to the other regions, the bias is slightly more negative, ranging between 0 and −6% between 15 and 40 km.

In the tropical region (right panel), fewest collocations are available. The effect of decreasing signal after having descended below the ozone maximum (which is at a higher altitude in the tropics) is clearly illustrated, as the variation increases with decreasing altitude. Likewise, the median shows an offset from the 0% difference in the tropics before that happens in the other areas.

3.2.5 Collocation criteria

Figure 9 confirms that the chosen collocation criteria are not introducing any biases. In fact, we could consider increasing the allowed difference in equivalent latitude, as we saw for subsets of the data that no clear deterioration was found when changing from 3 to 5 or 10 degrees. A more elaborated study focussing on the Polar area is to be carried out in the future.

Also, no evidence of a trend was observed when grouping the data by year (not shown), but perhaps this is masked by the flagging and or the chosen error regime.

4 Conclusions

Ground-/balloon based instruments can be used to bridge the gap between different satellite instruments, both in terms of technique and time. The ground-based observations often provide a long-term monitoring record with a high vertical resolution at a single location, whereas the satellite measurements are complementary as they can provide a global coverage with a limited life span. The comparison between data from satellite and ground-based instruments is a necessity to validate the retrievals and to monitor the performance of the instruments (Froidevaux et al., 2008; Hocke et al., 2007; Nardi et al., 2008; Jégou et al., 2008). The suite of ground-based and satellite retrievals together with models furthermore provides a unique tool to study atmospheric events and to detect trends (Ladstätter-Weißenmayer et al., 2007; Steinbrecht et al., 2006, 2009).

In this study we first have compared the ozone profiles from the current operational processor (version 5.00) with the previous version (4.02) by matching the datasets with ground and balloon based measurements. The validation results indicate that the two processing algorithms produce very similar results. The bias has improved in some areas, but a few more outliers are encountered. It was shown that a part of the outliers can be removed by filtering the profiles on negative and exceptionally large values. Improved quality flagging in future processor versions may overcome this problem.

Additionally, we have compared seven years of version 5.00 GOMOS ozone profiles with balloon sonde, lidar and microwave radiometer ozone measurements. Data were collocated using a maximum difference of 800 km, 3 degrees in equivalent latitude and 20 h in time (5 h above an altitude of 50 km). Lidar and microwave radiometer data were restricted to a maximum uncertainty of 30%, while the GOMOS profiles were filtered to exclude measurements with an error greater than 20%. For the dark limb observations, this resulted in 2115 collocated pairs with balloon soundings, 753 collocations with lidar observations and 669 collocations with microwave radiometer data.

ACPD
10, 8515–8551, 2010

The comparison shows that GOMOS profiles obtained from dark limb measurements are found to be of a high quality when the provided processing quality flag is properly takaen into account. Profiles measured under twilight conditions are of similar quality as dark limb measurements. However, the occurrence of outliers is higher. Care has to be taken in all cases when dealing with straylight contaminated profiles, which especially affect higher altitudes in the Polar region. Also in the mid-latitudes we can observe deviations from the validation data in the mesosphere. In the tropics there is a better match in the mesosphere between the validation instruments and the GOMOS measurements, but some large outliers are present. Overall, the ozone profiles are most similar (within a few percent) in the range 20 to 40 km, where the bias is moving towards the positive and the lowest good retrieval altitude increases when going from the poles to the equator.

Theoretically, observations of strong stars (visual magnitude ranging between −2 and 1) should result in profiles of have a higher quality (less noise) than observations of weak stars (magnitude between 1 and 4). However, for the GOMOS data within the selected error range (0–20%), we did not see any clear distinction between these two groups, but possibly that is related to the selection criteria applied here. The same is valid for the distinction between hot and cold stars. For instance, when extending the allowed error range to 100%, we see a large increase of the bias for the profiles obtained with cold stars.

Comparing the different azimuth ranges for the Line Of Sight (LOS), we can conclude that the median difference profiles are very similar and fewest outliers are observed using the back LOS configuration.

No evidence of a temporal trend was seen in the bias or occurrence of outliers, but it is likely that more profiles are rejected as the instrument ages. An analysis using a less strict data selection might be used to prove this. The next GOMOS processor version is expected to better deal with the increased dark charge of the detectors, reducing the amount of outliers and thus increasing the overall profile quality.

ACPD
10, 8515–8551, 2010

Acknowledgements. The authors wish to thank all institutes and investigators who have contributed the validation data used in this study. Sonde and microwave data were made available by the following institutes: Alfred Wegener institute for polar and marine research (Germany), Central aerological observatory (Russia), National research centre (France), Danish Meteorological Institute (Denmark), German weather service (Germany), Finnish meteorological institute (Finland), Hokkaido university (Japan), Institute of meteorology and climate research (Germany), Malaysian meteorological service (Malaysia), Meteorological and water research institute (Poland), MeteoSwiss (Switzerland), National institute for aerospace technology (Spain), National institute for air research (Norway), National institute for space research (Brazil), National institute of water and atmospheric research (New Zealand), NASA Wallops flight facility (United States of America), NOAA/ESRL Global monitoring division (United States of America), Royal Netherlands meteorological institute (The Netherlands), Royal meteorological institute (Belgium), South African weather service (South Africa), University of Bremen (Germany), University of Bern (Switzerland), University of Colorado (United States of America), University of La Reunion (France) and University of Rome (Italy).

We appreciate the comments of the anonymous reviewers which have helped to improve the quality of this manuscript.

References

Ballare, C. L., Scopel, A. L., Stapleton, A. E., and Yanovsky, M. J.: Solar ultraviolet-b radiation affects seedling emergence, DNA integrity, plant morphology, growth rate, and attractiveness to herbivore insects in Datura ferox, Plant Physiol., 112, 161–170, 1996.

Bass, A. M. and Paur, R. J.: The ultraviolet cross-sections of ozone – I. Measurements, in: Atmospheric ozone, edited by: Zeferos, C., Ghazi, A., and Reidel, D., Norwell, 606–610, 1985.

Bertaux, J.-L., Hauchecorne, A., Dalaudier, F., Cot, C., Kyrölä, E., Fussen, D., Tamminen, J., Leppelmeier, G. W., Sofieva, V. F., Hassinen, S., Fanton d'Andon, O., Barrot, G., Mangin, A., Théodore, B., Guirlet, M., Korablev, O., Snoeij, P., Koopman, R. M., and Fraisse, R.: First results on GOMOS/ENVISAT, Adv. Space Res., 33, 1029–1035, 2004.

Bogumil, K. Orphal, J. and Burrows, J. P.: Temperature dependent absorption cross sections measured with the SCIAMACHY satellite spectrometer – O_3 (version 2.0/August 2000),

http://www.iup.uni-bremen.de/gruppen/molspec/SCIA.html, last access: 8 November 2008, Molecular Spectroscopy and Chemical Kinetics group, University of Bremen, 2000.

Borchi, F. and Pommereau, J.-P.: Evaluation of ozonesondes, HALOE, SAGE II and III, Odin-OSIRIS and -SMR, and ENVISAT-GOMOS, -SCIAMACHY and -MIPAS ozone profiles in the tropics from SAOZ long duration balloon measurements in 2003 and 2004, Atmos. Chem. Phys., 7, 2671–2690, 2007, http://www.atmos-chem-phys.net/7/2671/2007/.

Brinksma, E. J., Bracher, A., Lolkema, D. E., Segers, A. J., Boyd, I. S., Bramstedt, K., Claude, H., Godin-Beekmann, S., Hansen, G., Kopp, G., Leblanc, T., McDermid, I. S., Meijer, Y. J., Nakane, H., Parrish, A., von Savigny, C., Stebel, K., Swart, D. P. J., Taha, G., and Piters, A. J. M.: Geophysical validation of SCIAMACHY Limb Ozone Profiles, Atmos. Chem. Phys., 6, 197–209, 2006, http://www.atmos-chem-phys.net/6/197/2006/.

Clerbaux, C., George, M., Turquety, S., Walker, K. A., Barret, B., Bernath, P., Boone, C., Borsdorff, T., Cammas, J. P., Catoire, V., Coffey, M., Coheur, P.-F., Deeter, M., De Mazière, M., Drummond, J., Duchatelet, P., Dupuy, E., de Zafra, R., Eddounia, F., Edwards, D. P., Emmons, L., Funke, B., Gille, J., Griffith, D. W. T., Hannigan, J., Hase, F., Höpfner, M., Jones, N., Kagawa, A., Kasai, Y., Kramer, I., Le Flochmoën, E., Livesey, N. J., López-Puertas, M., Luo, M., Mahieu, E., Murtagh, D., Nédélec, P., Pazmino, A., Pumphrey, H., Ricaud, P., Rinsland, C. P., Robert, C., Schneider, M., Senten, C., Stiller, G., Strandberg, A., Strong, K., Sussmann, R., Thouret, V., Urban, J., and Wiacek, A.: CO measurements from the ACE-FTS satellite instrument: data analysis and validation using ground-based, airborne and space-borne observations, Atmos. Chem. Phys., 8, 2569–2594, 2008, http://www.atmos-chem-phys.net/8/2569/2008/.

Deshler, T., Mercer, J. L., Smit, H. G. J., Stubi, R., Levrat, G., Johnson, B. J., Oltmans, S. J., Kivi, R., Thompson, A. M., Witte, J. C., Davies, J., Schmidlin, F. J., Brothers, G., and Sasaki, T.: Atmospheric comparison of electrochemical cell ozonesondes from different manufacturers, and with different cathode solution strengths: The Balloon Experiment on Standards for Ozonesondes, J. Geophys. Res., 11, D04307, doi:10.1029/2007JD008975, 2008.

Dupuy, E., Walker, K. A., Kar, J., Boone, C. D., McElroy, C. T., Bernath, P. F., Drummond, J. R., Skelton, R., McLeod, S. D., Hughes, R. C., Nowlan, C. R., Dufour, D. G., Zou, J., Nichitiu, F., Strong, K., Baron, P., Bevilacqua, R. M., Blumenstock, T., Bodeker, G. E., Borsdorff, T., Bourassa, A. E., Bovensmann, H., Boyd, I. S., Bracher, A., Brogniez, C., Burrows, J. P.,

Catoire, V., Ceccherini, S., Chabrillat, S., Christensen, T., Coffey, M. T., Cortesi, U., Davies, J., De Clercq, C., Degenstein, D. A., De Mazière, M., Demoulin, P., Dodion, J., Firanski, B., Fischer, H., Forbes, G., Froidevaux, L., Fussen, D., Gerard, P., Godin-Beekmann, S., Goutail, F., Granville, J., Griffith, D., Haley, C. S., Hannigan, J. W., Höpfner, M., Jin, J. J., Jones, A., Jones, N. B., Jucks, K., Kagawa, A., Kasai, Y., Kerzenmacher, T. E., Kleinbóhl, A., Klekociuk, A. R., Kramer, I., Küllmann, H., Kuttippurath, J., Kyrölä, E., Lambert, J.-C., Livesey, N. J., Llewellyn, E. J., Lloyd, N. D., Mahieu, E., Manney, G. L., Marshall, B. T., McConnell, J. C., McCormick, M. P., McDermid, I. S., McHugh, M., McLinden, C. A., Mellqvist, J., Mizutani, K., Murayama, Y., Murtagh, D. P., Oelhaf, H., Parrish, A., Petelina, S. V., Piccolo, C., Pommereau, J.-P., Randall, C. E., Robert, C., Roth, C., Schneider, M., Senten, C., Steck, T., Strandberg, A., Strawbridge, K. B., Sussmann, R., Swart, D. P. J., Tarasick, D. W., Taylor, J. R., Tétard, C., Thomason, L. W., Thompson, A. M., Tully, M. B., Urban, J., Vanhellemont, F., Vigouroux, C., von Clarmann, T., von der Gathen, P., von Savigny, C., Waters, J. W., Witte, J. C., Wolff, M., and Zawodny, J. M.: Validation of ozone measurements from the Atmospheric Chemistry Experiment (ACE), Atmos. Chem. Phys., 9, 287–343, 2009, http://www.atmos-chem-phys.net/9/287/2009/.

ESA: Record ozone loss during 2006 over South Pole, http://www.esa.int/esaCP/SEMQBOKKKSE_index_0.html, last access: 15 July 2009, 2006.

EO-PE (PLSO and MAO teams): Envisat mission extension beyond 2010 – scenario description. PE-RP-ESA-SA-205 1.0, 32 pp., 2007.

Froidevaux, L., Jiang, Y. B., Lambert, A., Livesey, N. J., Read, W. G., Waters, J. W., Browell, E. V., Hair, J. W., Avery, M. A., McGee, T. J., Twigg, L. W., Sumnicht, G. K., Jucks, K. W., Margitan, J. J., Sen, B., Stachnik, R. A., Toon, R. S., Fuller, R. A., Manney, G. L., Schwartz, M. J., Daffer, W. H., Drouin, B. J., Cofield, R. E., Cuddy, D. T., Jarnot, R. F., Knosp, B. W., Perun, V. S., Snyder, W. V., Stek, P. C., Thurstans, R. P., and Wagner, P. A.: Validation of Aura Microwave Limb Sounder stratospheric ozone measurements, J. Geophys. Res., 113, D15S20, doi:10.1029/2007JD008771, 2008.

Greenblatt, J. B., Jost, H.-J., Loewenstein, M., Podolske, J. R., Bui, T. P., Hurst, D. F., Elkins, J. W., Herman, R. L., Webster, C. R., Schauffler, S. M., Atlas, E. L., Newman, P. A., Lait, L. R., Müller, M., Engel, A., and Schmidt, U.: Defining the polar vortex edge from an N_2O:potential temperature correlation, J. Geophys. Res., 107(D20), 8268, doi:10.1029/2001JD000575, 2002.

Hocke, K., Kämpfer, N., Ruffieux, D., Froidevaux, L., Parrish, A., Boyd, I., von Clarmann, T., Steck, T., Timofeyev, Y. M., Polyakov, A. V., and Kyrölä, E.: Comparison and synergy of stratospheric ozone measurements by satellite limb sounders and the ground-based microwave radiometer SOMORA, Atmos. Chem. Phys., 7, 4117–4131, 2007, http://www.atmos-chem-phys.net/7/4117/2007/.

Jégou, F., Urban, J., de La Noë, J., Ricaud, P., Le Flochmoën, E., Murtagh, D. P., Eriksson, P., Jones, A., Petelina, S., Llewellyn, E. J., Lloyd, N. D., Haley, C., Lumpe, J., Randall, C., Bevilacqua, R. M., Catoire, V., Huret, N., Berthet, G., Renard, J. B., Strong, K., Davies, J., Mc Elroy, C. T., Goutail, F., and Pommereau, J. P.: Technical Note: Validation of Odin/SMR limb observations of ozone, comparisons with OSIRIS, POAM III, ground-based and balloon-borne instruments, Atmos. Chem. Phys., 8, 3385–3409, 2008, http://www.atmos-chem-phys.net/8/3385/2008/.

Koti, S., Reddy, K. R., Reddy, V. R., Kakani, V. G., and Zhao, D.: Interactive effects of carbon dioxide, temperature, and ultraviolet-B radiation on soybean (Glycine max L.) flower and pollen morphology, pollen production, germination, and tube lengths, J. Exp. Bot., 56, 725–736, 2005.

Ladstätter-Weißenmayer, A., Kanakidou, M., Meyer-Arnek, J., Dermitzaki, E. V., Richter, A., Vrekoussis, M., Wittrock, F., and Burrows, J. P.: Pollution events over the East Mediterranean: Synergistic use of GOME, ground-based and sonde observations and models, Atmos. Environ., 41, 7262–7273, 2007.

Liu, X., Chance, K., Sioris, C. E., and Kurosu, T. P.: Impact of using different ozone cross sections on ozone profile retrievals from Global Ozone Monitoring Experiment (GOME) ultraviolet measurements, Atmos. Chem. Phys., 7, 3571–3578, 2007, http://www.atmos-chem-phys.net/7/3571/2007/.

Luchnik, N. V.: On the mechanism of production of chromosomal aberrations by ultraviolet radiation, Mutat. Res., 27, 295–298, 1975.

McDermid, I. S., Godin, S. M., and Lindqvist, L. O.: Ground-based laser DIAL system for long-term measurements of stratospheric ozone, Appl. Optics, 29, 3603–3612, 1990.

McDermid, I. S., Bergwerff, J. B., Bodeker, G., Boyd, I. S., Brinksma, E. J., Connor, B. J., Farmer, R., Gross, M. R., Kimvilakani, P., Matthews, W. A., McGee, T. J., Ormel, F. T., Parrish, A. S. U., Swart, D. P. J., Tsou, J. J., Wang, P. H., and Zawodny, J.: OPAL: Network for the Detection of Stratospheric Change Ozone Profiler Assessment at Lauder, New Zealand, 1, Blind intercomparison, J. Geophys. Res., 103, 28683–28692, 1998.

Meijer, Y. J., van der A, R. J., van Oss, R. F., Swart, D. P. J., Kelder, H. M., and Johnston, P. V.: Global Ozone Monitoring Experiment ozone profile characterization using interpretation tools and lidar measurements for intercomparison, J. Geophys. Res.-Atmos., 108, ACH 4-1–ACH 4-11, doi:10.1029/2003/JD003498, 2003.

Meijer, Y. J., Swart, D. P. J., Allaart, M., Andersen, S. B., Bodeker, G., Boyd, I., Braathen, G., Calisesi, Y., Claude, H., Dorokhov, V., von der Gathen, P., Gil, M., Godin-Beekmann, S., Goutail, F., Hansen, G., Karpetchko, A., Keckhut, P., Kelder, H. M., Koelemeijer, R., Kois, B., Koopman, R. M., Kopp, G., Lambert, J.-C., Leblanc, T., McDermid, I. S., Pal, S., Schets, H., Stubi, R., Suortti, T., Visconti, G., and Yela, M.: Pole-to-pole validation of Envisat GOMOS ozone profiles using data from ground-based and balloon sonde measurements, J. Geophys. Res., 109, D23305, doi:10.1029/2004JD004834, 2004.

Milchunas, D. G., King, J. Y., Mosier, A. R., Moore, J. C., Morgan, J. A., Quirk, M. H., and Slusser, J. R.: UV radiation effects on plant growth and forage quality in a shortgrass steppe ecosystem, Photochem. Photobiol., 79, 404–410, 2004.

Molina, M. J. and Rowland, F. S.: Stratospheric sink for chlorofluoromethanes: chlorine atom-catalysed destruction of ozone, Nature, 249, 810–812, 1974.

Müller, R. and Günther, G.: A generalized form of Lait's modified potential vorticity, J. Atmos. Sci., 60, 2229–2237, 2003.

NDACC lidar working group, www.ndacc-lidar.org, last access: 14 January 2010, 2009.

Nardi, B., Gille, J. C., Barnett, J. J., Randall, C. E., Harvey, V. L., Waterfall, A., Reburn, W. J., Leblanc, T., McGee, T. J., Twigg, L. W., Thompson, A. M., Godin-Beekmann, S., Bernath, P. F., Bojkov, B. R., Boone, C. D., Cavanaugh, C., Coffey, M. T., Craft, J., Craig, C., Dean, V., Eden, T. D., Francis, G., Froidevaux, L., Halvorson, C., Hannigen, J. W., Hepplewhite, C. L., Kinnison, D. E., Khosravi, R., Krinsky, C., Lambert, A., Lee, H., Loh, J., Massie, S. T., McDermid, I. S., Packman, D., Torpy, B., Valverde-Canossa, J., Walker, K. A., Whiteman, D. N., Witte, J. C., and Young, G.: Initial validation of ozone measurements from the High Resolution Dynamics Limb Sounder, J. Geophys. Res.-Atmos., 113, D16S36, doi:10.1029/2007JD008837, 2008.

Nisbet, E.: Earth monitoring: Cinderella science, Nature, 450, 789–790, 2007.

Orphal, J.: A critical review of the absorption cross sections of O_3 and NO_2 in the 240-790 nm region, part I: Ozone, ESA technical note MO-TN-ESA-GO-0302, 2002.

Orphal, J.: A critical review of the absorption cross-sections of O_3 and NO_2 in the ultraviolet and visible, J. Photoch. Photobio. A, 157, 185–209, 2003.

Roscoe, H. K., Jones, A. E., and Lee, A. M.: Midwinter start to Antarctic ozone depletion: Evidence from observations and models, Science, 278, 93–96, 1997.

Sofieva, V. F., Kan, V., Dalaudier, F., Kyrölä, E., Tamminen, J., Bertaux, J.-L., Hauchecorne, A., Fussen, D., and Vanhellemont, F.: Influence of scintillation on quality of ozone monitoring by GOMOS, Atmos. Chem. Phys., 9, 9197–9207, 2009, http://www.atmos-chem-phys.net/9/9197/2009/.

Steinbrecht, W., Claude, H., Schönenborn, F., McDermid, I. S., Leblanc, T., Godin, S., Song, T., Swart, D. P. J., Meijer, Y. J., Bodeker, G. E., Connor, B. J., Kämpfer, N., Hocke, K., Calisesi, Y., Schneider, N., de la Noë, J., Parrish, A. D., Boyd, I. S., Brühl, C., Steil, B., Giorgetta, M. A., Manzini, E., Thomason, L. W., Zawodny, J. M., McCormick, M. P., Russell, J. M., Bhartia, P. K., Stolarski, R. S., and Hollandsworth-Frith, S. M.: Long-term evolution of upper stratospheric ozone at selected stations of the Network for the Detection of Stratospheric Change (NDSC), J. Geophys. Res.-Atmos., 111, D10308, doi:10.1029/2005JD006454, 2006.

Steinbrecht, W., Claude, H., Schönenborn, F., McDermid, I. S., Leblanc, T., Godin-Beekmann, S., Keckhut, P., Hauchecorne, A., van Gijsel, J. A. E., Swart, D. P. J., Bodeker, G. E., Parrish, A., Boyd, I. S., Kämpfer, N., Hocke, K., Stolarski, R. S., Frith, S. M., Thomason, L. W., Remsberg, E. E., von Savigny, C., Rozanov, A., and Burrows, J. P.: Ozone and temperature trends in the upper stratosphere at five stations of the network for the detection of atmospheric composition change, Int. J. Remote Sens., 30, 3875–3886, 2009.

Tamminen, J., Karhu, J., Kyrölä, E., Hassinen, S., Kyrö, E., Karpechko, A., and Piacentini, E.: GOMOS Ozone Profiles at High Latitudes: Comparison with Marambio and Sodankylä Sonde Measurements, in: Atmosphere and Climate, Springer, Berlin Heidelberg, 47–54, 2006.

Thompson, A. M., Witte, J. C., McPeters, R. D., Oltmans, S. J., Schmidlin, F. J., Logan, J. A., Fujiwara, M., Kirchhoff, V. W. J. H., Posny, F., Coetzee, G. J. R., Hoegger, B., Kawakami, S., Ogawa, T., Johnson, B. J., Vömel, H., and Labow, G.: Southern Hemisphere Additional Ozonesondes (SHADOZ) 1998–2000 tropical ozone climatology 1. Comparison with Total Ozone Mapping Spectrometer (TOMS) and ground-based measurements, J. Geophys. Res., 108(D2), 8238, doi:10.1029/2001JD000967, 2003a.

Thompson, A. M., Witte, J. C., Oltmans, S. J., Schmidlin, F. J., Logan, J. A., Fujiwara, M., Kirchhoff, V. W. J. H., Posny, F., Coetzee, G. J. R., Hoegger, B., Kawakami, S., Ogawa, T., Fortuin, J. P. F., and Kelder, H. M.: Southern Hemisphere Additional Ozonesondes (SHADOZ)

1998–2000 tropical ozone climatology 2. Tropospheric variability and the zonal wave one, J. Geophys. Res., 108, 8241, doi:10.1029/2002JD002241, 2003b.

Urbach, F.: Ultraviolet radiation and skin cancer of humans, J. Photoch. Photobiol. B, 40, 3–7, 1997.

van der Leun, J. C. and de Gruijl, F. R.: Influence of ozone depletion on human health, in: UV-B radiation and ozone depletion, edited by: Tevini, M., Lewis Publishers, Boca Raton (FL), 95–123, 1993.

Verronen, P. T., Kyrölä, E., Tamminen, J., Funke, B., Gil-López, S., Kaufmann, M., López-Puertas, M., von Clarmann, T., Stiller, G., Grabowski, U., and Höpfner, M.: A comparison of night-time GOMOS and MIPAS ozone profiles in the stratosphere and mesosphere, Adv. Space Res., 36, 958–966, 2005.

Table 1. Overview of analysed data subsets per parameter.

Parameter	Subset name	Range
Illumination condition (solar zenith angle)	bright limb	0° to 90°
	twilight limb	90° to 108°
	dark limb	108° to 180°
Star visual magnitude	strong stars	−2 to +1
	weak stars	+1 to +4
Star temperature	cold stars	1000 K to 7000 K
	hot stars	7000 K to 40 000 K
Line Of Sight (LOS) azimuth angle	back LOS	−10° to +10°
	slant LOS	+10° to 45°
	side LOS	+45° to 90°
Latitude (absolute values)	polar region	66.5° to 90°
	mid-latitudes	23.5° to 66.5°
	tropics	0° to 23.5°
Collocation criteria	within 800 km and 20 h	$\Delta x \leq 800$ km & $\Delta t \leq 20$ h
	within 400 km and 10 h	$\Delta x \leq 400$ km & $\Delta t \leq 10$ h
	within 200 km and 5 h	$\Delta x \leq 200$ km & $\Delta t \leq 5$ h

ACPD
10, 8515–8551, 2010

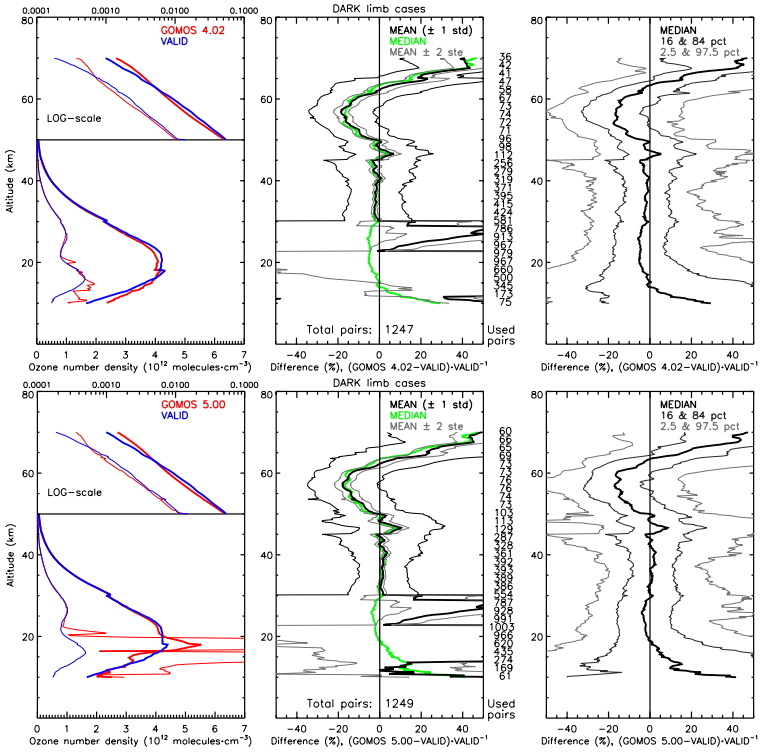

Fig. 1. GOMOS 4.02 (top) and 5.00 (bottom) versus validation data. Left panels show the ozone number density as a function of altitude, with the GOMOS profiles in red and the validation data in blue (mean and standard deviation in thick and thin lines respectively). The ozone concentration is plotted on a log-scale for the upper 30 km. The middle panels show the difference between GOMOS and the validation data (with respect to the validation data) in percentage as a function of altitude. The green line shows the median difference profile, the black lines the mean (thick black line) ±1 standard deviation (thin lines) and the grey lines show the mean ±2 standard errors. On the right side of the middle panel the number of collocated pairs is shown, with the total number of used pairs at the bottom of the plot. The right panel shows the median difference (thick black line) together with the 16 and 84 percentiles (dark grey lines) and the 2.5 and 97.5 (light grey lines) percentiles.

ACPD
10, 8515–8551, 2010

GOMOS ozone profile validation using ground-based measurements

J. A. E. van Gijsel et al.

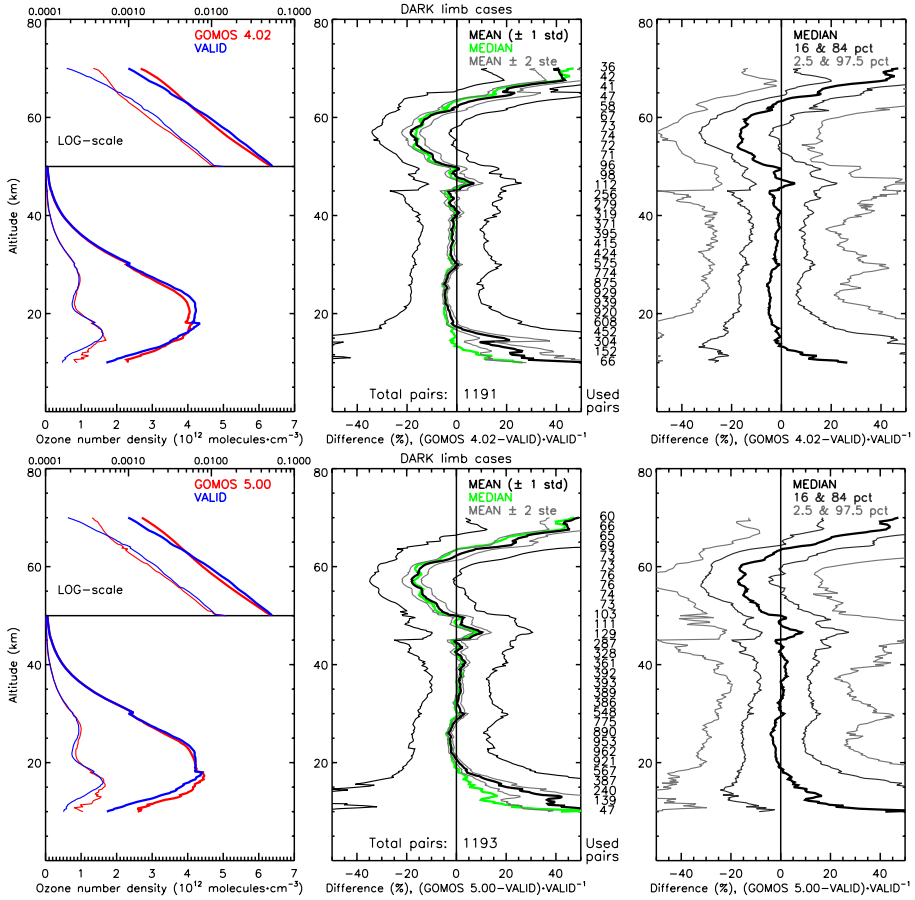

Fig. 2. As Fig. 1, except filtered for ozone values below 0 and above 19 to 13 molecules per cm^3 and with some Thule, Dumont d'Urville and Legionowo cases removed.

ACPD
10, 8515–8551, 2010

GOMOS ozone profile validation using ground-based measurements

J. A. E. van Gijsel et al.

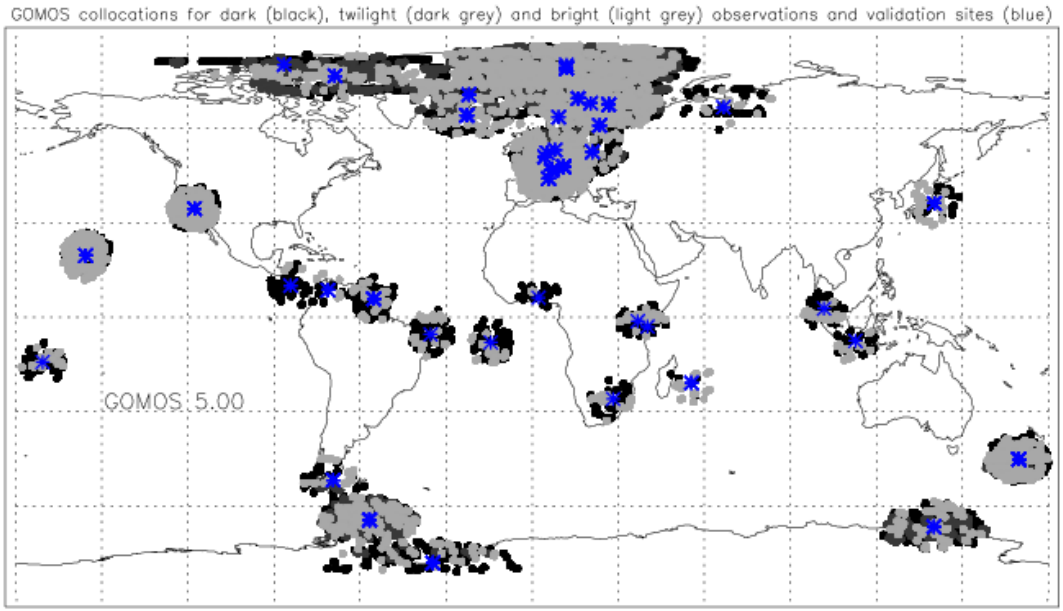

Fig. 3. Global overview of collocated measurements available in this study. GOMOS measurements in black (dark limb observations), dark grey (twilight conditions) and light grey (bright limb observations) circles together with the validation sites plotted as blue asterisks.

ACPD

10, 8515–8551, 2010

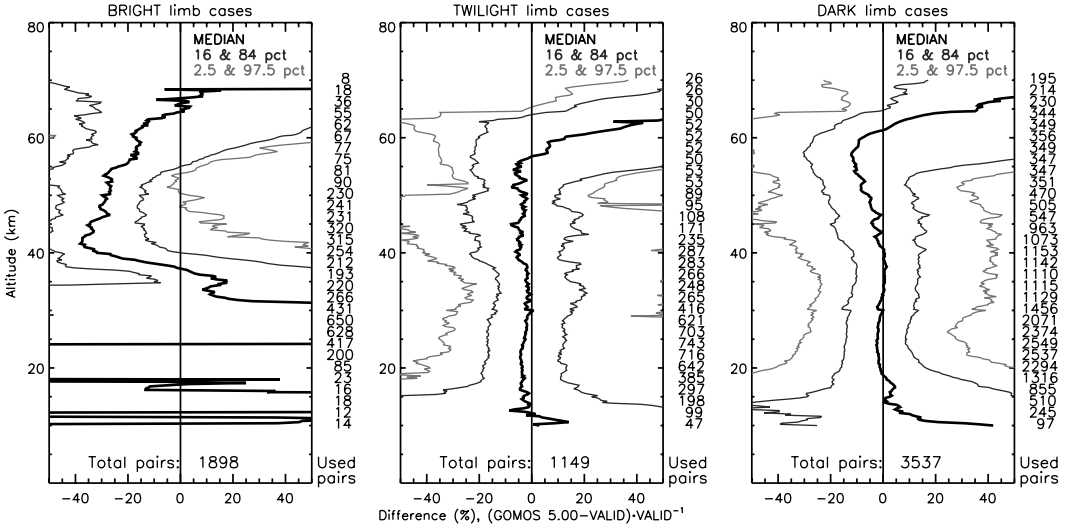

Fig. 4. Validation results for the different limb illumination conditions. Left panel: bright limb; middle panel: twilight limb; right panel: dark limb cases. All plots show the median difference (thick black line) between GOMOS and the validation data together with the 16 and 84 percentiles (thin dark grey lines) and the 2.5 and 97.5 percentiles (thin light grey lines). On the right side of each panel is the number of collocated pairs used for the corresponding altitude.

ACPD
10, 8515–8551, 2010

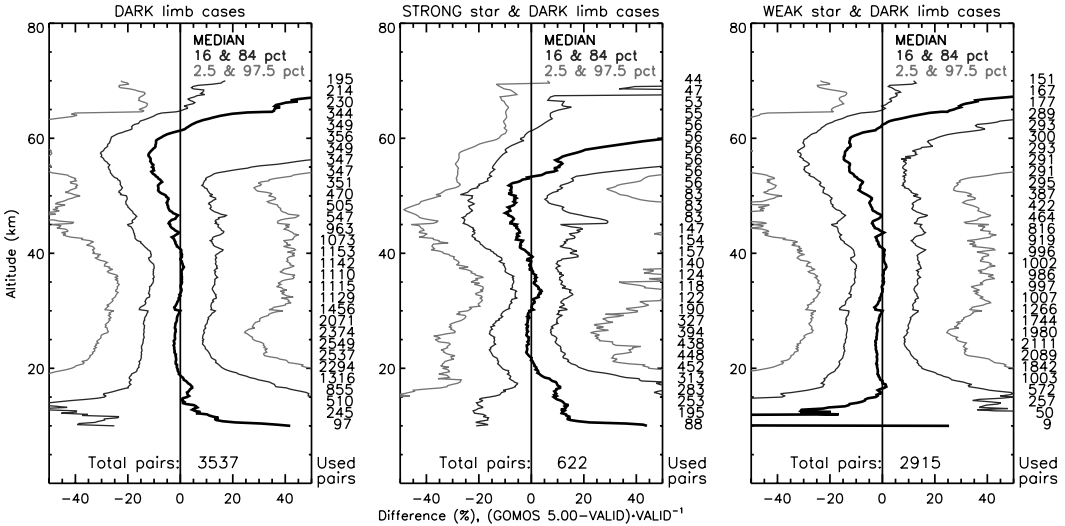

Fig. 5. As Fig. 4, but showing validation results for different star magnitude ranges. Left panel: all cases together; middle panel: observations using strong stars; right panel: observations using weak stars.

ACPD
10, 8515–8551, 2010

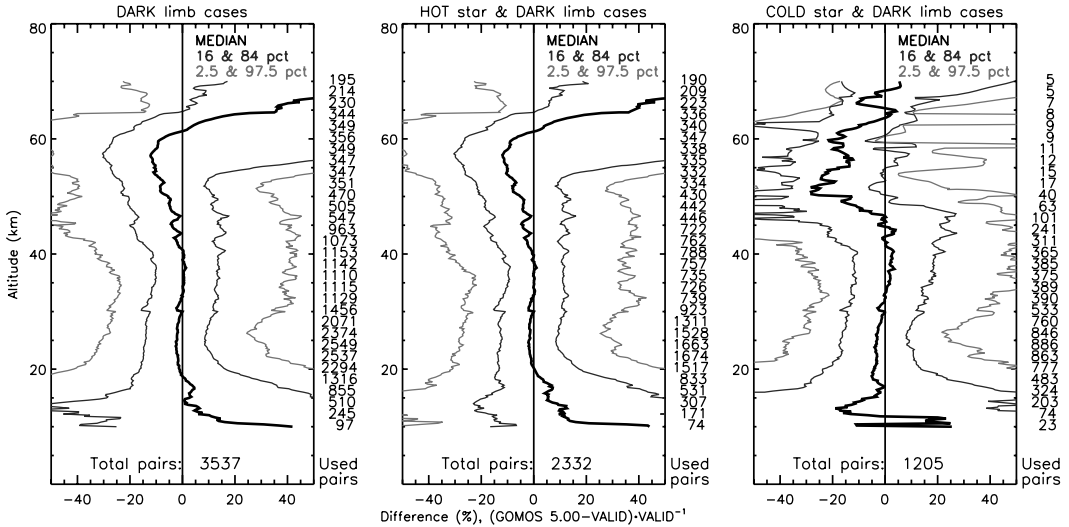

Fig. 6. As Fig. 4, but showing validation results for different star temperature groups. Left panel: all cases together; middle panel: observations of hot stars; right panel: observations of cold stars.

ACPD
10, 8515–8551, 2010

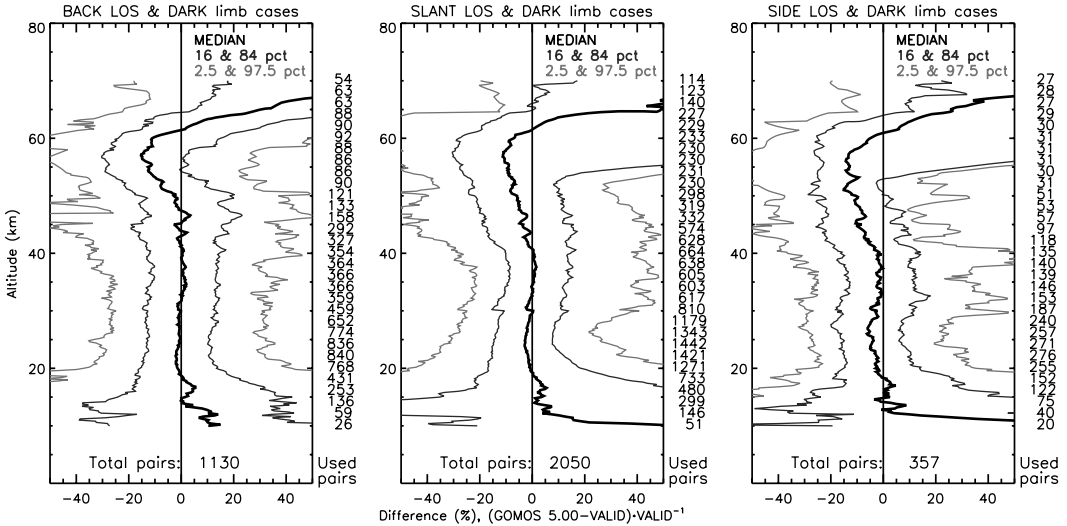

Fig. 7. As Fig. 4, except showing the cases grouped by line of sight azimuth angles. Left panel: backward viewing (−10° to 10°); middle panel: slant viewing (10° to 45°); right panel: sideward viewing (45° to 90°).

ACPD
10, 8515–8551, 2010

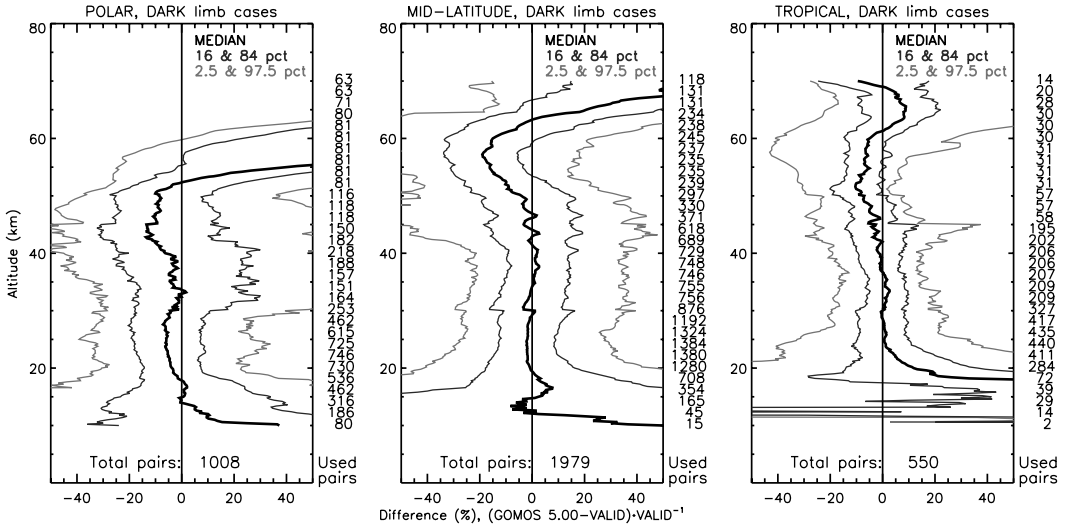

Fig. 8. As Fig. 4 showing the validation results for the different latitude regions. Left panel: polar cases; middle panel: mid-latitude regions; right panel: tropical region.

ACPD
10, 8515–8551, 2010

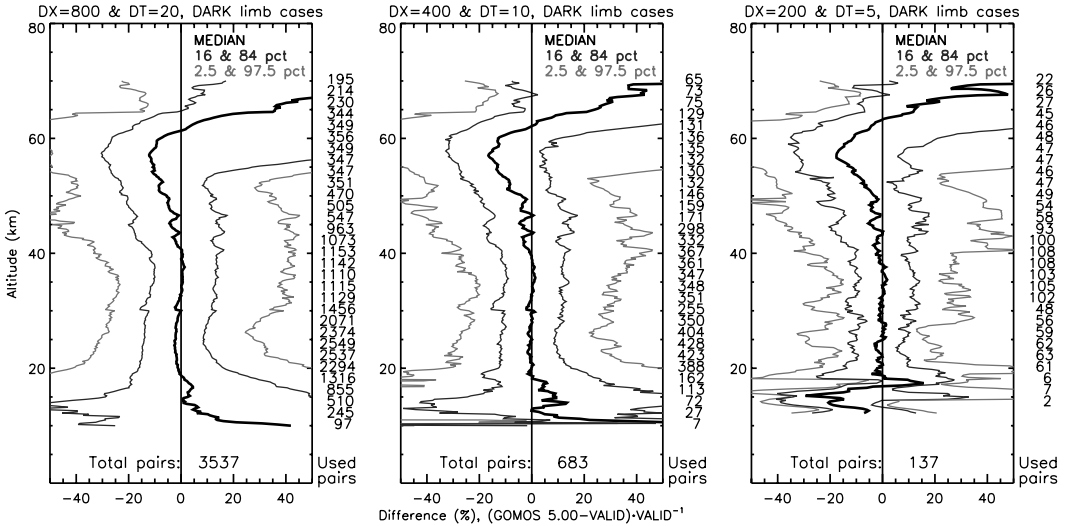

Fig. 9. As Fig. 4, here showing the effect of making the collocation criteria stricter. Left panel: cases with a maximum difference of 800 km and 20 h; middle panel: 400 km and 10 h maximum difference; right panel: cases fulfilling a 200 km and 5 h maximum difference.

ACPD
10, 8515–8551, 2010